# SHAPING OF PARABOLIC CYLINDRICAL MEMBRANE REFLECTORS FOR THE DART PRECISION TEST BED

C. White[1] (AIAA Member), M. Salama[1] (AIAA Associate Fellow), M. Dragovan[1], Hatheway[2] (AIAA Senior Member) J. Schroeder[1], D. Barber[1], J. Dooley[1]

[1]Jet Propulsion Laboratory, 4800 Oak Grove Drive, Pasadena, CA 91109-8099
[2]Alson E. Hatheway, Inc. Suite 400, 595 East Colorado Blvd, Pasadena, CA 91101

## ABSTRACT

The DART is a new telescope architecture consisting of two cylindrical parabolic reflectors. The system is ideally suited to using tensioned membranes for the reflective surfaces, owing to the zero Gaussian curvature of a cylindrical parabola. In this paper we investigate a technique for shaping the membranes which uses curved boundary elements to achieve coarse shaping, and a pair of precision rails shaped by moments and forces at the ends, and lightly pushed into the surface, to provide fine shape control. Nonlinear finite element analyses show that the rails have a large control authority, and establish that the membrane shape is somewhat different from the rail shape. An experimental testbed has been constructed to demonstrate the ideas using a 70cm by 80cm membrane reflector. Key mechanical design aspects are discussed which lead to a highly adjustable and precise membrane surface.

## BACKGROUND

There are many indications that future space-based telescopes and large aperture antennas will require the use of lightweight gossamer structures. Primarily this is because in the long term membrane structures have the best chance of delivering the hundreds or thousands of square meter apertures demanded by future missions. Traditional architectures using stiff monolithic reflectors or even segmented deployable reflectors will exceed launch vehicle lift capabilities for even modestly sized apertures.

Membrane reflectors enjoy another significant advantage besides weight: economy. Because their large reflecting areas do not need to be ground into precise shapes, nor do the shapes need to be precisely tested before launch, they can potentially be placed on orbit very quickly and much less expensively.

A new concept in membrane reflective telescopes for the Far-IR has been proposed in the form of the DART.[1,2,3] The DART is a system of two cylindrical parabolic reflectors, each one of which produces a line focus, but when properly oriented, produces a point focus. The system is ideally suited to using tensioned membranes for the reflective surfaces, owing to the zero Gaussian curvature of a cylindrical parabola.

In this research, we propose a shape control idea for the precise shaping of zero Gaussian curvature membrane surfaces. The control concept uses a pair of parallel rods bent into the proper curvature by end forces and pushed lightly into the membrane surface. Using both nonlinear finite element models and a program of experimental measurements made on a precision testbed, the goal is to produce a membrane surface shape with minimal surface root mean square error for an aperture of 50cm. The lessons learned from these investigations can be applied to realistic telescope and antenna designs of larger sizes.

The paper begins with a nonlinear structural analysis of a single precision rail, whereby it is established that a system of end moments and axial forces can shape a slender rod into a parabolic curve with less than one micron of error – for both on-axis and off-axis shapes of interests – even under the action of distributed contact forces. The paper continues with details on the finite element analyses used for surface shape prediction and presents a few results that illustrate the abilities of the analysis. That section also outlines a plan for computing the proper rail shapes to achieve optimal surface precision. The paper concludes with a description of the test hardware.

## FLEXIBLE PRECISION RAILS FOR SHAPE CONTROL

Owing to the unidirectional curvature of cylindrical geometries, a membrane surface can be developed by enforcing the desired curvature along two edges of the membrane, for instance by using 'rigid' clamping elements having the desired curvature, and lightly stretching the membrane parallel to the axis of the cylinder. The stretching removes any wrinkles and provides a geometric stiffness normal to the surface.

To make refinements to the membrane shape, we propose that a pair of 'precision rails', each having

the proper curved shape, be pushed lightly into the membrane surface. These rails run parallel to the clamped edges, and are located some distance away from the clamp faces. By using flexible rails supported at the ends by mechanisms that adjust the bending moments and axial force, the curvature of the rail can be changed. The shape of the rail then influences the shape of the membrane.

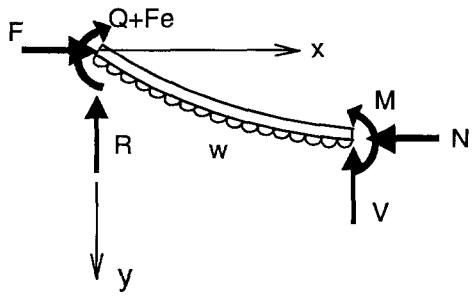


Figure 1 Free body of flexible beam in deformed configuration. Beam has length L, bending stiffness EI.

The question of whether the precision rail can be deformed into a parabolic shape is of fundamental interest. Consider the system of forces acting on a section of the precision rail shown in Figure 1. The end moment is Q, and the axial force F is assumed to act with eccentricity e. There is a uniform load per unit length of value w, which is representative of the contact force between the membrane and the rail. The nonlinear differential equation of beam deflection is easily written as

$$\frac{y''}{(1+y'^2)^{3/2}} = -\frac{1}{EI}\left[-\frac{wL}{2}x + Fy + Q + Fe + \frac{wx^2}{2}\right] \quad (1)$$

Although various approximations and simplifications may be made, Equation 1 is a difficult differential equation to solve in closed-form. It is known that an analytical solution can be made using elliptic integrals. Despite the appeal of having been extensively studied, any solution of an elliptic integral ultimately relies on tabulated, or numerical, values. Instead of pursuing the elliptical integral solution, a purely numerical solution of the differential equation has been made using the Runge-Kutta method.

If the target is to form the precision rail to exactly the prescription of the parabolic reflecting surface, the end moment Q and axial force F need to be determined, assuming the eccentricity e is fixed and beam properties L, EI are known. Any of the general optimization algorithms can be applied to this problem, where the design variables are of course Q and F and the objective function is the root mean square of residual error between the precision rail shape and the prescription parabola.

The results of the optimization are provided in Table 1 for a beam length of 80 cm, diameter of 6.0 mm and elastic modulus of 200 GPa. A representative plot of the residuals along the length of the rail is shown in Figure 2. The very significant result of these calculations is that a system of end moments and axial forces is theoretically capable of forming the precision rail into a parabolic shape with sub-micron precision.

A similar analysis has been performed for the off-axis reflector geometry. One difference is that the end moments are necessarily different, and unequal shear reactions are needed to balance the moments. Nevertheless, the same conclusions apply: the precision rail can be formed into the off-axis parabolic shape with submicron precision. Table 2 demonstrates this.

A critical issue is shape robustness in the presence of small deviations in end moment and axial force. Such small deviations could realistically be present in any hardware design due to temperature effects or creep. At the very least, it is prudent to know how sensitive the basic concept is to such deviations. To investigate this, deviations of one percent are applied to both Q and F independently, while keeping the other at its previously optimal value. The results are presented in Table 3.

These maximum residuals scale nearly linearly with error in F and Q, so it can be concluded that to keep the maximum residual to less than one micron, F must be kept within approximately 0.17%, and Q within 0.004%, or one part in 600 and one part in 25000.

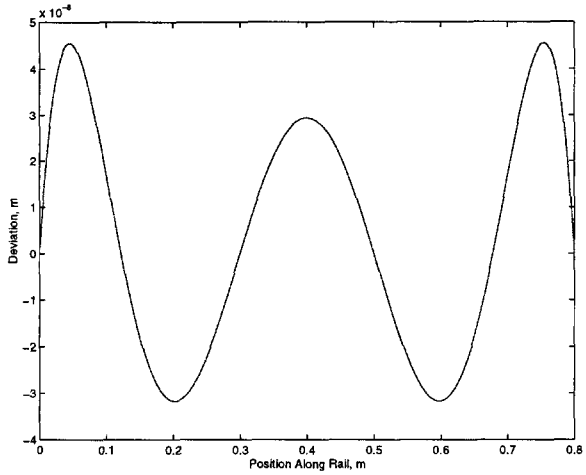


Figure 2 Residuals after computing optimal F and Q for the case w=1 N/m. The range on the ordinate is -0.04 μm to 0.05 μm.

Table 1 Required F and Q as contact load w varies, on-axis reflector geometry.

| w (N/m) | F (N) | Q (N·m) |
|---|---|---|
| 0 | 5.086648 | 5.10334862 |
| 1 | 8.134648 | 5.10334862 |
| 5 | 20.32666 | 5.10334830 |
| 10 | 35.56668 | 5.10334775 |

Table 2 Required F and Q for off-axis reflector geometry. $Q_L$ and $Q_S$ are the larger and smaller end moments.

| W N/m | F (N) | $Q_L$(N·m) | $Q_S$(N·m) | Max residual (μm) |
|---|---|---|---|---|
| 0 | -0.029167 | 3.673825 | 2.925055 | 0.235 |
| 1 | 4.732026 | 3.671935 | 2.926861 | 0.088 |
| 5 | 23.77683 | 3.664373 | 2.934088 | 0.052 |
| 10 | 47.58291 | 3.654912 | 2.943130 | 1.3 |

Table 3 Effects of small deviations in F and Q, for the nominal case, e=0.00, w=0. $F_N$ , $Q_N$ are the optimal values from Table 1.

| F (N) | Q (N·m) | Max. residual (microns) |
|---|---|---|
| $F_N$ - 1% | $Q_N$ | 5.8 |
| $F_N$ + 1% | $Q_N$ | 5.7 |
| $F_N$ | $Q_N$ - 1% | 265 |
| $F_N$ | $Q_N$ + 1% | 265 |

## REFLECTOR SHAPE MODELING

Geometrically nonlinear finite element models can be used to predict the surface shape of a tensioned membrane. As a rule of thumb, geometrically nonlinear analysis is required if deflections exceed the thickness of the membrane. Certainly if there are areas of wrinkling in the membrane, such an analysis is required for accurate shape predictions. Contact between the precision rails and the membrane is a central feature of the shaping idea and good, and various, contact algorithms are a fundamental requirement in the finite element code. The ability to analyze orthotropic or anisotropic material properties is not generally a concern if the membrane is an electroformed metal (highly isotropic), but may become a primary concern for certain types of polymers.

The IMOS[4] integrated mechanical-thermal-optical and control analysis program is available for optical systems analysis. However, it was not seriously considered for this work because it lacks every single one of the abilities outlined above.

The LS-DYNA3D[5] computer program was chosen because of the code's ability to handle rigid and flexible bodies, the wide choice of contact algorithms, and the ease of computing nonlinear geometrical response, in particular wrinkling, through explicit numerical integration of the equations of motion. This is a code the first two authors have used extensively and effectively for large displacement and highly nonlinear analyses[7,8,9]. Because the problems are always solved using dynamic relaxation, there are never any numerical problems with convergence.

The nominal finite element model is a rectangular membrane with dimensions 70cm by 80cm, of 50 μm thick electroformed copper foil. The membrane is modeled with quadrilateral shells. The membrane is divided into two parts: a central 50cm square region representing the aperture, and the remaining area around the aperture. The nodes along two edges of the membrane are attached to curved clamps of aluminum, of dimensions 2cm by 3cm by 70 cm, modeled with solid brick elements. For reasons of manufacturability, the clamps are constructed (and modeled) with mating surfaces that are arcs of circular curves, not parabolas. The precision rails are stainless steel precision ground bars of 6.0mm diameter, modeled with 3-d beam elements. The precision rails are defined in a reference, stress-free, configuration to have the desired shape of the parabolic surface, and are initially not touching the

membrane. A Cartesian coordinate system is assigned to the problem such that X-axis is parallel to the clamp faces, Z-axis is normal to the clamp faces, and Y-axis is normal to the membrane surface at the vertex.

The baseline model uses 2cm square shell elements and 7.6 mm long beam elements. With 1292 shells, 816 solids, 212 beams, and 2979 nodes, this is a fairly coarse mesh, but it solves quickly. Models with finer discretization are considered below. Although LS-DYNA has a number of reduced-integration shell elements which are computationally cheap, as well as a resultant beam element, experience has shown that the fully-integrated elements are required for this problem.

The stretching preload force is applied with concentrated loads at two locations on one of the clamps, while the other clamp is properly restrained at symmetric points. The precision rails have prescribed displacement boundary conditions assigned to their end nodes such that the rotations and axial translations can be held to zero while the normal direction translations can be prescribed to move the rails into contact with the membrane.

Surface figure error is computed with the MATLAB program by fitting a conic surface to the deformed nodal coordinates computed in LS-DYNA and computing the root-mean-square of the residuals. Because changes in radius of the surface shape can be corrected through telescope focus, we have allowed the best-fit algorithm to compute the optimal parabolic cylinder of any radius of curvature and report the radius along with the rms error. In all cases, the residual is fit only within the square 50 cm aperture.

## THE POISSON EFFECT

If the membrane is connected to the clamp so there is no relative motion, the membrane cannot contract at the clamp boundary per the Poisson effect as it stretches. As a consequence, transverse stresses are established, and the membrane 'dogbones' while simultaneously pushing up normal to its surface. This effect is shown in Figure 3 with displacements exaggerated by a factor of 2500. The amount that a single node at the center of the aperture moves in the Y-direction is a linear function of the amount of stretching force: for 100N total force, the node moves 27.2 μm. As seen in Table 4, the surface error is a nonlinear function of preload, at least in part due to the clamps being circular rather than parabolic.

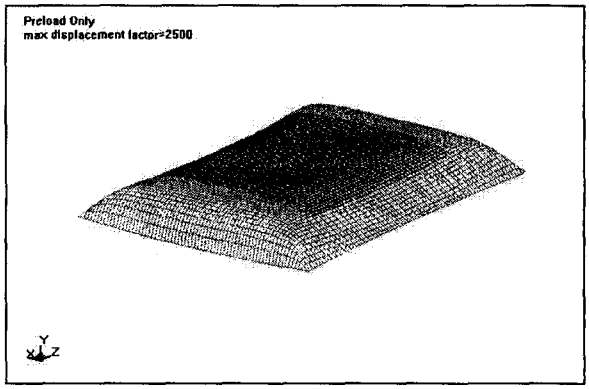


Figure 3 Computed shape of a rectangular membrane lightly tensioned along Z-axis.

Table 4 Normal direction displacement and root mean square surface error for various preload forces.

| Preload (N) | Y-displacement (μm) | RMS Error (μm) |
|---|---|---|
| 0 | 0 | 1.51 |
| 20 | 5.5 | 1.33 |
| 60 | 16.5 | 1.47 |
| 100 | 27.7 | 1.57 |

## PRECISION RAIL EFFECT

The precision rails are positioned 56cm apart, a spacing that was chosen early in the investigation simply so that the rails are located outside the aperture. The rails are pushed into the reflective side of the membrane. It was also somewhat arbitrarily decided to push the rails a distance so that the vertex nodes of the membrane just under the rails were displaced 25μm from the preload equilibrium position.

The character of the deformed surface is shown in Figure 4 and Figure 5. It is clear that the membrane maintains a relatively good figure in the center of the aperture, but that the errors increase towards the free edges of the membrane.

The optimal parabolic cylindrical surface was fit to the simulation data with a root mean square error of 5.50μm, and a radius of curvature of 3.06155m. The shape of the residual error over the aperture is shown in Figure 6. It is evident that if one cuts the residuals surface parallel to X-axis, a standard W-curve is obtained, whereas a cut parallel to Z-axis gives a curve flat in the middle and rising up monotonically at each end.

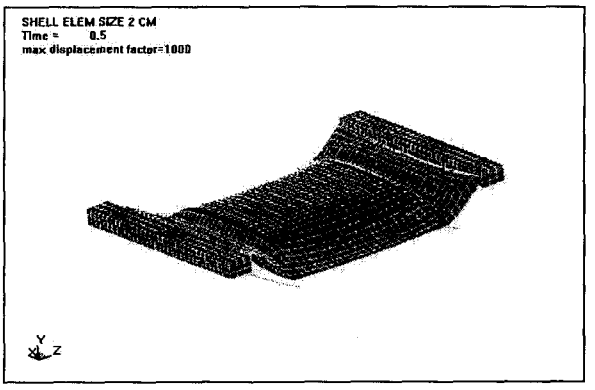


Figure 4 The deformed shape is shown with displacements magnified 1000 times.

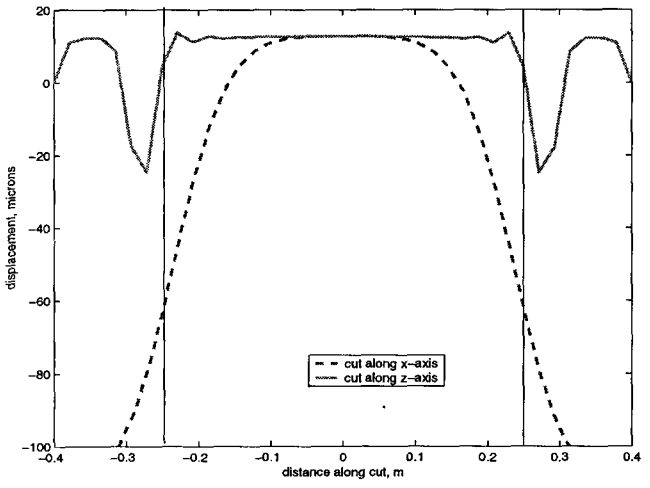


Figure 5 Displacements computed along two lines, one parallel to the clamp faces, and one normal to the clamp faces, both passing through the center of the aperture. The vertical lines at ±0.25 m represent the edges of the 50cm square aperture.

As the rail pushes into the membrane, there is a contact force distributed along the rail, deforming the rail. The computed total contact force is shown in Figure 8. A parabolic curve is fit to the deformed shape of the precision rail and results in root-mean-square residuals of 0.11μm and a radius of curvature of 3.04882m. The familiar W-curve is shown in Figure 7.

It follows that the contact force from the membrane tends to flatten the precision rail – increasing its radius from 3.048m to 3.04882m. The change is less than 0.03 percent, and seems to indicate that a 6mm diameter rail would be stiff enough. It also follows that the membrane flattens slightly.

## OPTIMAL SURFACE SHAPE

These baseline analysis results make it clear that the membrane and the precision rail do not share the same shape. In fact, in these analyses the precision rails are not reducing the surface errors. The results suggest that separating the rails a little more and perhaps using a rail with a smaller curvature would improve the shape. A smaller curvature could be achieved by either prescribing a rotation to the ends of the rails, or translating each end inwards. If either of these is done, the rails push deeper into the surface, and this in and of itself increases the figure error.

The degrees of freedom that are of interest to setting the rail shape are the end rotation (moment), the end axial translation (axial force), and the Y position (push distance). At this point, a logical approach to investigating the precision rails is to use an optimization or feedback control algorithm. The objective function is the surface error root mean square value, and the design variables are end rotation, axial translation, and Y position.

One software tool capable of performing such an analysis is the optimization software LS-OPT[6]. LS-OPT employs the response surface methodology and is particularly efficient when executed in the parallel mode. Automatic execution of the root-mean-square calculations by MATLAB is possible by passing the *m-file* name as a command line option. This approach is currently being pursued.

## MESH CONVERGENCE

The effects of increasing mesh density are shown in Figure 9 and Figure 10, and Table 5. Both shell element and solid element mesh densities are increased.

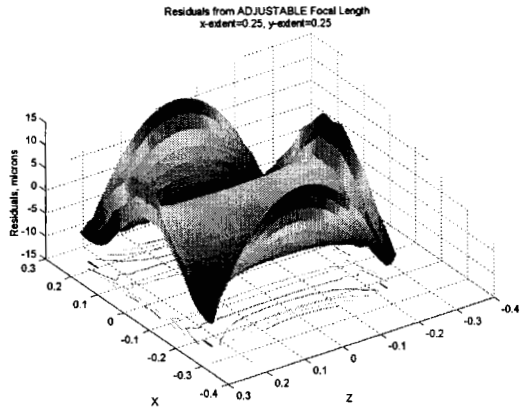


Figure 6 Three dimensional surface of residuals.

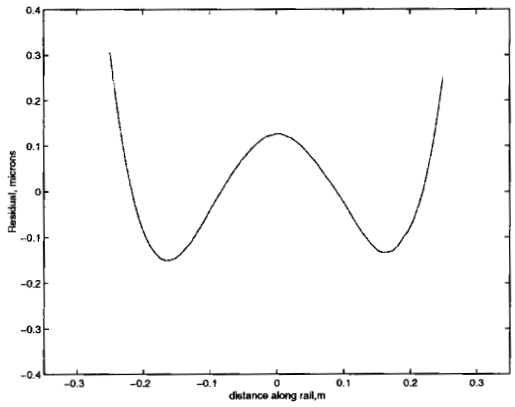


Figure 7 residual of precision rail

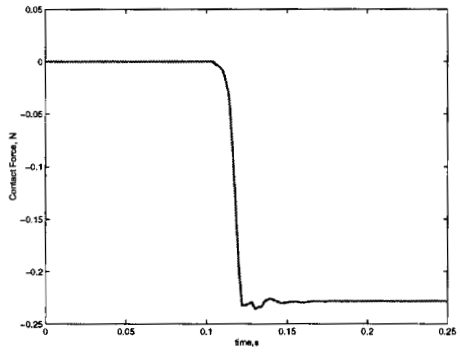


Figure 8 Contact force time history for one precision rail, integrated along the entire length of contact.

Table 5 Variation of key response quantities with increasing mesh densities.

| Shell Size | Nodes | Execution time | Radius (m) | RMS Error (μm) |
|---|---|---|---|---|
| 2cm | 2979 | 3 hrs | 3.06155 | 5.50 |
| 1cm | 12781 | 12 hrs | 3.05600 | 3.77 |
| 0.5cm | 69659 | >106 hrs. | 3.05533 | 2.90 |

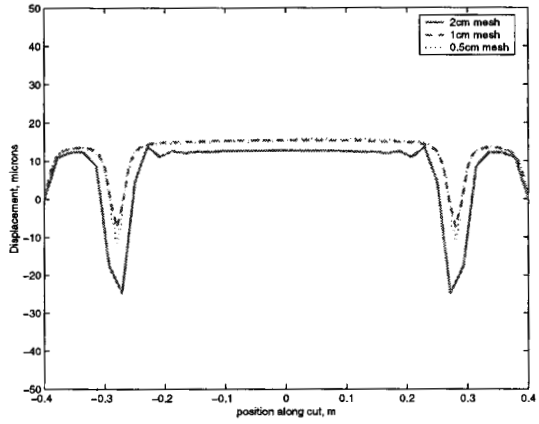


Figure 9 Effects of mesh density on displacements along a line cut taken through aperture center parallel to Z-axis.

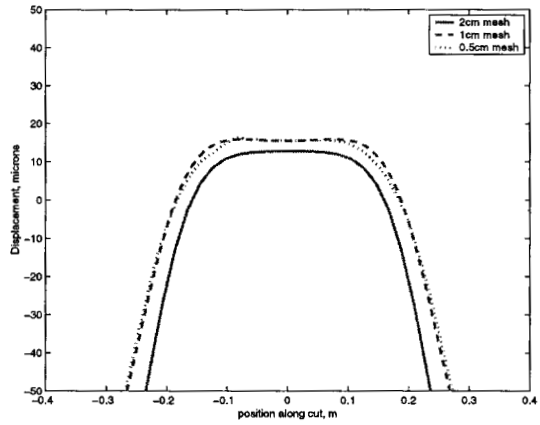


Figure 10 Effects of mesh density on displacements along a line cut taken through aperture center parallel to X-axis.

## PRECISION REFLECTOR TESTBED

A testbed for a single on-axis reflector has been developed to demonstrate the shaping accuracies attainable for parabolic cylindrical reflectors. Through measurements of the surface shape, the testbed provides corroboration for the computational models, and by adding the off-axis reflector, can be extended to demonstrate the imaging performance of the telescope. Specifically excluded from the design requirements are requirements on the mass, the ability to operate at cryogenic temperatures, the suitability for space flight, the ability to deploy, and the ability to efficiently scale this specific design to larger sizes.

The hardware consists of four major components:

1. the 80cm x 70cm membrane
2. a frame structure that reacts the stretching forces.
3. aluminum clamps that form the coarse curvature and deliver the preload stretching load
4. a pair of precision rails

A diagram of the design is shown in Figure 11. Note the alignment mechanisms at each clamp bar that adjust the membrane preload and boundary displacements. The alignment and shaping adjustability is a key feature of the testbed.

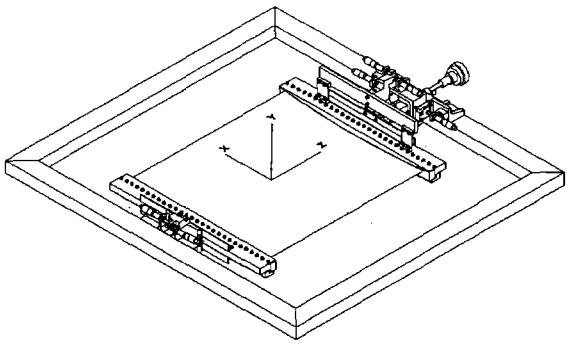

Figure 11 The preload frame is constructed of 5cm x 7.5cm aluminum tubing. It reacts the tension load and provides the ability to align the membrane prior to placing the precision rails. It also supports the two precision rails (not shown).

### MEMBRANE

Electroformed copper foil is used for the membrane. Copper is used because of its highly reflective properties at IR wavelengths, its extremely uniform mechanical properties, and the fact that it lacks a glass transition temperature.

The foil has a nominal thickness of 50 μm. Rolls of the foil were obtained from two manufacturers and coupon samples were subjected to uniaxial testing following ASTM E 345-93. The average mechanical properties from three tests on each material are reported in Table 6.

Table 6 Electroformed Cu foil mechanical properties

| Batch | Thickness (μm) | Modulus (GPa) | Poisson's Ratio |
|---|---|---|---|
| 1 | 62.74 | 113 | 0.34 |
| 2 | 65.28 | 109 | 0.24 |

### FRAME AND CLAMP

Sensitivity analyses were used to understand the effects of misalignment in each of the six degrees of freedom of one of the boundary clamps. Using a preliminary model of a 50cm square membrane that omitted the shaping rails, and holding one of the two clamps fixed, the figure error for misalignments in each translational direction and each rotational direction of the other clamp was computed. The misalignment was arbitrarily assumed to be 100 microns in translation and 1.7 mrad in rotation. Results in Table 7 confirm intuition that misalignments in Tx, Ry and Rz have the largest influence. These correspond to shearing, toe-in, and twisting alignment errors. One of the more interesting cases is Preload + Tx, and the wrinkled shape is shown in Figure 12. Based on these results, we have designed the testbed to be adjustable only in these degrees of freedom.

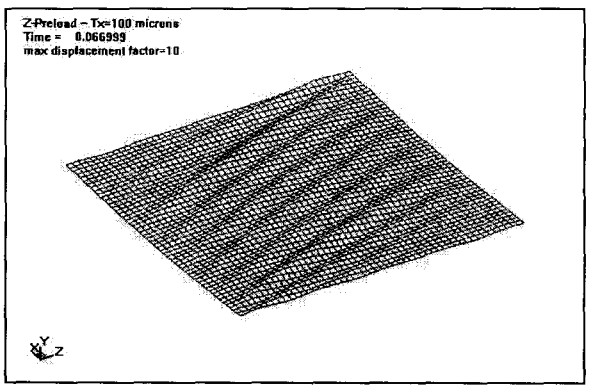


Figure 12 Membrane surface wrinkles due to shearing of the clamp boundaries in the X-direction.

Table 7 Surface shape root mean square error (μm) computed for six degrees of clamp misalignment.

| Pre-load only | Pre-load + Tx | Pre-load + Ty | Pre-load + Tz | Pre-load + Rx | Pre-load + Ry | Pre-load + Rz |
|---|---|---|---|---|---|---|
| 5.8 | 236 | 7 | 25 | 8 | 82 | 21 |

The preload is applied at two locations on the clamp bars, and is adjustable at one end through a spring-regulated fine-thread screw mechanism. Preload force is monitored with a load cell. Frictional interfaces are minimized in the design, and flexures are used throughout. Adjusting mechanisms were designed to minimize coupling among adjustments, and incorporate pairs of precision micrometers with a resolution of 0.1 μm arranged in opposition so that the adjustments can be locked out.

## PRECISION RAILS

The rails are formed with precision ground 6.0 mm diameter stainless steel rods, available commercially as a standard order item. Such rods are typically used for linear bearings. The rails span the width of the membrane and are supported at each end by adjusting mechanisms attached to the preload frame and allow the rails to be aligned with respect to the frame.

An important feature of the rail design is that the forces and moments that shape the rails are equilibrated by a parallel blade element. The blade element, also made of stainless steel, decouples the shaping forces and moments from the reaction frame, and allows for greater precision in shaping the rail. Micrometers acting through levers deliver the axial force and end moment to shape the rail. The shaping mechanism is shown in Figure 13.

The somewhat large lever arm required on the moment adjustment is due to the total rotational displacement required on the end of the rail, the high precision required on that displacement (1:25000 as described above), and limits on the magnitude of axial force that can be resisted by a precision micrometer. The solution which satisfied these requirement substituted a 1μm resolution, 50mm travel micrometer for the 0.1μm precision micrometers used in the other alignment devices.

Load cells are incorporated to monitor the applied loads. Due to the high sensitivity in rail shape to end force and moment magnitudes, these measurements are not the sole basis for adjusting the shape of the rail. Other metrics such as optical image quality or the position of several key points on the membrane surface are much more convenient in practice.

The rotational bearings used in the design are a potential source of imprecision and randomness in positioning. High precision low radial-play angular contact bearings are specified.

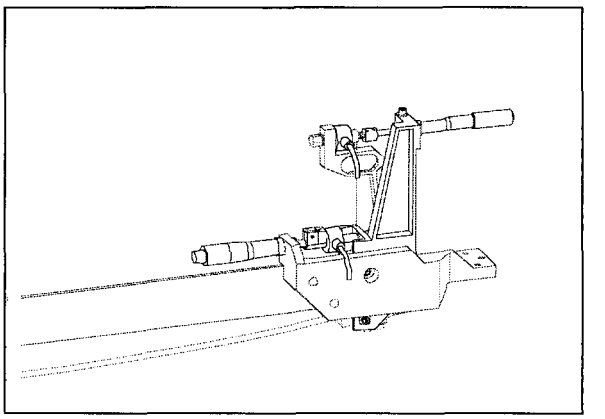

Figure 13 Micrometers and levers are used to apply the bending moment and axial forces to the precision rail.

## METROLOGY

A four-stage course-to-fine measurement process is being developed. The first stage uses collimated light to approximately focus the reflector. A second stage uses a profilometer to scan along critical lines or perhaps the entire surface. A resolution of 100 nm is expected with the profilometer. The third uses an infrared interferometer and a nulling lens to measure the entire surface at a resolution of 30 nm RMS. The fourth and final stage, as needed, will use a smaller nulling lens at a greater resolution to focus in on areas of greatest interest.

## CONCLUSION


## ACKNOWLEDGEMENTS

The research described in this paper was carried out by the Jet Propulsion Laboratory, California Institute of Technology, and its collaborators under a contract with the National Aeronautics and Space Administration. The discussions and contributions of Shari and Jim Day for advice regarding the LS-DYNA3D software are greatly appreciated.

## REFERENCES


1. Dragovan, M. 2000, '*Low Mass Density Wide Field FarIR/Sub-millimeter Telescope Systems*', astro-ph/0001241 (http://xxx.lanl.gov/abs/astro-ph/0001241)

2. Dragovan, M. 2002, '*DART System for FarIR/Submillimeter membrane telescopes*', Proeeedings SPIE Conference on Astronomical Telescope and Instrumentation, Waikoloa, HI, Vol. 4849, Aug, 2002.

3. Tolomeo, J., G. Cross, B. Sable, T. Decker, D. Putnam, T. Jamieson, M. Dragovan, A. Chmielewski, J. Dooley, 2002, '*Design and test of a prototype DART system*', Proeeedings SPIE Conference on Astronomical Telescope and Instrumentation, Waikoloa, HI, Vol. 4849, Aug, 2002.

4. *Integrated Modeling of Optical Systems User's Manual*, JPL Publication 98-12, Rev. B, March 2002

5. J. O. Hallquist, *LS-DYNA Keyword User's Manual*, LS-DYNA Version 960, Livermore Software Technology Corporation, Livermore, CA, March 2001.

6. N. Stander, *LS-OPT User's Manual Version 1*, Livermore Software Technology Corporation, Livermore, CA.

7. M. Salama, Fang, H., Lou, M., *Resistive Deployment of Inflatable Structures Using Velcro*, Journal of Spacecraft and Rockets, Vol. 39, No. 5, 2002, pp.711-716.

8. M. Salama, White, C., Leland, S., *Ground Demonstration of a Spinning Solar Sail Deployment Concept*, Journal of Spacecraft and Rockets, Vol. 40, No. 1, 2003.

9. C. White, S. Day, *Analysis and Experimentation for the Aerial Deployment of Planetary Balloons*, IEEE Aerospace Conference, Big Sky, MT, 2003.